Chemical Engineering & Processing: Process Intensification 129 (2018) 181–189

Contents lists available at ScienceDirect

Chemical Engineering & Processing: Process Intensification

journal homepage: www.elsevier.com/locate/cep

A fundamental analysis of the influence of the geometrical properties on the effective thermal conductivity of open-cell foams

Mauro Bracconi, Matteo Ambrosetti, Matteo Maestri, Gianpiero Groppi, Enrico Tronconi*

Laboratory of Catalysis and Catalytic Processes, Dipartimento di Energia, Politecnico di Milano, via La Masa 34, Milano, Italy

ARTICLE INFO

Keywords:
Open-cell foams
Effective solid thermal conductivity
Optimized structure
Process intensification

ABSTRACT

Structured catalysts have been proposed as a suitable solution for the efficient management of strongly exo- and endothermic processes. Among these structures, open-cell foams are considered as one of the most promising candidates as catalyst supports. In this work, we investigated the heat transfer in the solid matrix of open-cell foams by means of 3D numerical simulations carried out on virtually reconstructed structures. The totally interconnected solid matrix promotes high heat transfer rates because the conduction in the solid matrix is the main contribution to the heat transport. Our analysis reveals that the void fraction is the controlling parameter for the performances of the structures. An engineering correlation for the effective solid thermal conductivity has been derived, enabling a rational design of the foam geometry. Moreover, we analyzed the effect of the ratio between the node and strut diameters. We found that it has a strong influence on the heat conduction performance. High ratios penalize the heat transfer due to the reduced strut cross-section area at fixed porosity. On the other hand, an advanced design with a node-to-strut diameter ratio close to one can enhance the effective heat conductivity of open-cell foams up to 30%, improving the reactor performances compared to conventional open-cell foams.

1. Introduction

Heat management and temperature control are pivotal aspects in the design and operability of several catalytic processes, enabling safe operation and increased process selectivity and yield. Conventional packed bed shell-and-tube reactors suffer from poor radial heat transfer, which is typically limited by the convective transport in the gas phase. High flow velocities are required to promote the energy transfer implying, as a drawback, long catalytic reactors and high pressure drops. To overcome these limitations, structured catalysts are widely acknowledged as a potential and promising solution for the efficient management of strongly exo- and endothermic processes [1,2], since the heat transfer is mainly governed by conduction in the solid matrix. In this view, open-cell foams are considered among the most promising candidates as catalyst supports. They are a cellular material consisting of random and reticulated open cells surrounded by solid interconnected ligaments. The open structure makes open-cell foams permeable to the fluid flow, which can stream through the pores. Moreover, the high void fraction strongly reduces the pressure drops [3]. The presence of the solid ligaments in cross-flow increases the mixing and the gas-solid transfer rates [4,5]. The totally interconnected solid matrix is expected to enhance axial and radial heat transfer, being thermal conduction in the solid matrix the main contribution to the heat transport, which can be up to more than 97% in the case of highly conductive metal foam-air systems, as revealed by Calmidi et al. [6] and later confirmed by Bianchi et al. [7] and Aghaei et al. [8]. In this perspective, the adoption of highly conductive metallic foams (i.e. copper, aluminum or nickel) would result in a boost of the conductivity of the catalytic support with beneficial effects in highly endothermic (e.g. steam reforming) and exothermic (e.g. selective oxidation, methanation, Fischer–Tropsch) reactions. The high heat transfer rates enabled by the conductive mechanism are expected to minimize the presence of hot-spot and to prevent thermal-shock limitations allowing for the design of compact reactors [9]. This is crucial in view of process intensification in exothermic and endothermic processes preserving the catalyst and enhancing the performances of the system. The accurate analysis of the heat conduction mechanism and the description by means of lumped parameters, i.e. effective conductivity, is of utmost importance for the rational design of industrial reactors. Experimental and theoretical works aiming to evaluate the stagnant conductivity have been carried out by several researchers [10–16]. Many of the experimental works aimed to analyze the thermal conductivity of open-cell foams saturated with air or other fluids were carried out in static conditions imposing a temperature gradient on the face of the foam or a

* Corresponding author.
E-mail address: enrico.tronconi@polimi.it (E. Tronconi).

https://doi.org/10.1016/j.cep.2018.04.018
Received 11 March 2018; Received in revised form 6 April 2018; Accepted 16 April 2018
Available online 25 April 2018

Nomenclature

Latin letters

A	foam area (m^2)
d_c	cell diameter (m)
d	strut diameter (m)
d_s	minimum strut diameter (m)
$d_{n,s}$	diameter at strut-node intersection (m)
h	height of spherical cap (-)
k_s	thermal conductivity of the solid material (W/m/K)
k_{eff}	effective thermal conductivity of the foam (W/m/K)
J	heat flux (W/m^2)
L	foam side length (m)
P_i	coefficients of the polynomial (-)
R	ratio between diameter at strut-node intersection and minimum strut diameter (-)
S	foam bounding box area (m^2)
T	temperature (K)
z	axial strut coordinate (m)
z_s	coordinate of the strut-node junction (m)

Greek letters

ε	void fraction (-)
γ	Plateau's angle (°)
τ	tortuosity (-)

heat flux. Moreover, this problem has been tackled by means of three-dimensional numerical simulations accurately accounting for the complex foam microstructure as well. Bianchi et al. [7] and Fan et al. [17] carried out simulations on tomographically-reconstructed geometries. Their investigations are confined to a small range of void fractions, characteristic of the commercial metal foams, between 0.89 and 0.95. Moreover, the size of the analyzed sample is constrained by the maximum dimension achievable in the reconstruction procedure. Randrianalisoa et al. [18] simulated the pure heat conduction in virtual structures generated by means of Voronoi tessellation. The struts are modeled with a non-constant strut diameter whose variation is assumed to be parabolic. However, the adequacy of the geometrical model with respect to the real foams structure and the peculiar material distribution between struts and nodes was not assessed. Ranut [19] extensively reviewed the gas and solid effective thermal conductivity models for highly porous metal foams. Several empirical and theoretical models have been proposed, however most of them are confined to very high void fractions. Those analyses showed that the Lemlich model [20] adequately describes the stagnant effective thermal conductivity at high porosities. In the lower void fraction range, the experimental data are widely scattered and their engineering correlation is still an open question.

A detailed characterization of the effective solid thermal conductivity of foams over the entire range of porosities is missing. Most of the experimental and numerical activities are confined to a narrow range of geometrical properties and foam materials. A comprehensive and parametric analysis of the stagnant heat conduction in a broad range of void fraction and geometrical properties is therefore required.

In this work, we analyze the effective stagnant heat conductivity in the solid matrix by means of three-dimensional numerical simulations carried out on virtually-generated structures fully retaining all the geometrical properties of real foam structures [21]. We neglect the radiation contribution which has been investigated in [14,22,23] and, however, in the case of highly conductive foams is generally at least one order of magnitude lower than the contribution associated with conduction through the interconnected struts [8]. This analysis requires the generation of digital reconstructions representative of the complex geometrical structure of real foams. Recently, we proposed a procedure for the generation of accurate and realistic virtual foams [21]. The generation procedure is based on the Voronoi tessellation which is widely acknowledged as a realistic first guess for the foam skeletal structure. The proper description of the geometry is of utmost importance for the assessment of the heat transfer properties. In particular, a dedicated model [24] has been exploited to account for the distribution of the solid material between nodes and struts, and for the accurate description of the variation of the strut diameter along the axis. The overall procedure [21] has been validated in a broad range of different porosities, pores per inch (PPI) and strut shapes, reaching a very satisfactory agreement for the geometrical properties. By employing the virtual structures, the effect of different geometrical properties, i.e. porosity, cell size, can be studied in a systematic and highly reproducible way with precise control on the morphological and geometrical parameters of the supports. After a comprehensive validation of the virtual geometries against experimental data, the fundamental simulations pointed out that the stagnant effective heat conductivity strongly depends on the void fraction, whereas a negligible effect of the cell diameter is obtained. We derived an engineering correlation for open-cell foams following the approach employed by Bianchi et al. [25] for the description of periodic ordered structures (POCS).

Recently, novel additive manufacturing techniques, e.g. selective electron beam melting (SEBM) or selective laser melting (SLM), are receiving attention due to their capability of producing metal-based 3D structures with a well-defined geometry as recently shown by Freund and co-workers [25,26]. In this perspective, the limitations and constraints on the geometry of the foam imposed by the current manufacturing techniques can be easily overcome. Thus, we extended the previous analysis to the optimization of the foam structure with the goal of improving the heat transfer performance. The controlling resistance to the heat conduction at fixed porosity is expected to be located in the middle of the strut, where the smallest cross-sectional area is observed. In this work, we quantify the effect of different ratios between the cross-sectional area evaluated in the middle of the strut and in the nodes as already carried out by Bianchi et al. [25] for periodic ordered structures. We analyzed three different ratios elucidating that a high ratio hinders the structure performances. This analysis paves the way for the rational design of open-cell structures with improved and optimized effective conduction properties, which hold a huge potential for process intensification in the chemical process industry.

2. Methods and models

In this Section, we briefly review the virtual reconstruction procedure which generates the virtual foam models ready for the simulation of the heat transfer properties starting from easy accessible geometrical inputs, i.e. the cell diameter and the void fraction. Specific attention is devoted to the description of simplified models used for the estimation of the first guess of the node and strut geometry required for the generation of the foam samples. Finally, we analyze the meshing procedure and we introduce the equations required for the estimation of the stagnant thermal conductivity.

2.1. Virtual reconstruction

The foam structure is generated by means of a Voronoi-tessellation procedure. The initial seeds required by the algorithm are obtained by means of a random packing of spheres of cell diameter size. The packed bed is generated by means of a discrete element method [27]. Once the

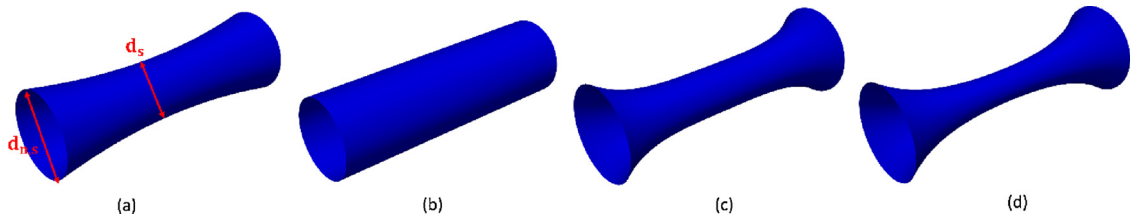

Fig. 1. Strut inserted in the structure for a foam with d_c = 1.5 mm and ε = 0.8 generated using the original TKKD geometrical model (a) and the modified model with R = 1 (b), R = 2 (c) and R = 3 (d).

spheres are settled, the centers of the internal portion of the packing are extracted. The sphere centers represent the position of the foam cells. The Voronoi algorithm generates the skeleton of foam according to the provided set of seeds building the unit cells constituting the geometrical skeleton of the structure. The detailed description of the strut and node geometry is a key aspect of the procedure. In this work, we modify the previously developed procedure of digital foam reconstruction [21] to deal with arbitrary distributions of the solid material between nodes and struts, introducing the additional degree of freedom required by the purpose of the optimization.

2.1.1. Models of node-strut geometry

The virtual foam reconstruction requires an appropriate and detailed description of the node and strut geometries, which are generated starting from simplified models based on a tetrakaidekahedron (TKKD) cell. In this work, we define as strut and node diameters the value estimated in the middle of the strut and at the junction between node and strut as reported in Fig. 1(a). The node and strut diameters are related by a ratio defined as $R = d_{n,s}/d_s$. We distinguish three different geometrical models according to desired strut-node material distribution of the final foam samples. In particular, we consider the TKKD model with parabolic profile of the strut perimeter proposed by Ambrosetti et al. [24], which accurately describe the geometrical properties of real foams, and two modified versions able to deal with an arbitrary ratio and with a ratio equal to one, respectively.

2.1.1.1. Original TKKD model with parabolic strut profile. The generation of foams according to the original virtual reconstruction procedure [21] requires an initial estimation of node and strut diameters carried out with the original TKKD model proposed by Ambrosetti et al. [24]. This fully-theoretically grounded model employs a simple unit cell coupled with the accurate and detailed description of the node and strut geometries for the prediction of the geometrical properties of foams. In particular, the unit cell is assumed to be a tetrakaidekahedron. A second order parabolic variation of the strut diameter is further assumed to account for the non-uniform distribution of the material between strut and node. Moreover, a condition of continuity and differentiability of the strut profile is imposed at the junction between the node and the strut; in particular, the derivative should be equal to tan(γ/2), where γ is the Plateau's angle [28]. The strut diameter is calculated from a third-order algebraic equation that imposes the porosity in the idealized cell; all the other variables can be evaluated in cascade. More details can be found in [24]. This model has been extensively validated against experimental data for the geometrical properties of several foams with satisfactory results [24] and the adequacy of the estimation for the virtual reconstruction has been previously assessed [21]. An example of a strut geometry is shown in Fig. 1(a).

The hypotheses and assumptions imposed for the development of the geometrical model result in a variable R ratio with respect to the foam void fraction. Fig. 2 shows the trend of the ratio upon changing the solid fraction. A ratio higher than 2.5 is predicted at high void fractions, which gradually decreases on decreasing porosity approaching almost 1 at $(1 - \varepsilon) = 0.3$.

2.1.1.2. TKKD model with variable ratio between strut and node. We extend the original TKKD model to account for different solid distributions between nodes and struts. The distribution of the solid material is controlled by the ratio between the diameter of the strut, i.e. the value in the middle of the strut profile (d_s), and of the node, i.e. the diameter of the strut at the junction with the node ($d_{n,s}$). As in the original model, we consider the following assumptions [24]:

- Tetrakaidekahedral unit cell.
- Continuity and differentiability of the strut profile and the strut/node junction.
- The solid material loaded in the structure is totally distributed between struts and nodes.

Differently from [24], we link the node and strut diameters by the ratio $R = d_{n,s}/d_s$. A 4th order profile of the strut is now considered, as proposed in literature by Liebscher et al. [29], for the evolution of the strut diameter along the axis as reported in Eq. (1). A fourth order polynomial is required to introduce the additional parameter necessary to define the ratio.

$$d(z) = P_1 z^4 + P_2 z^2 + P_3 \tag{1}$$

where d is the diameter of the strut, z is the axial coordinate and P_i are the coefficients of the polynomial. By imposing the continuity and differentiability of the profile at the node/strut junction following the approach previously proposed in [24] and by assigning the ratio between node and strut diameters (R) the value of the P_i are totally defined and the expression is reported in Eqs. (2)–(4).

$$P_1 = \frac{d_s(R-1) - \frac{z_s \sin\frac{\gamma}{2}}{1-h}}{2z_s^4} \tag{2}$$

$$P_2 = \frac{\frac{d_s}{2}(R-1) - P_1 z_s^4}{z_s^2} \tag{3}$$

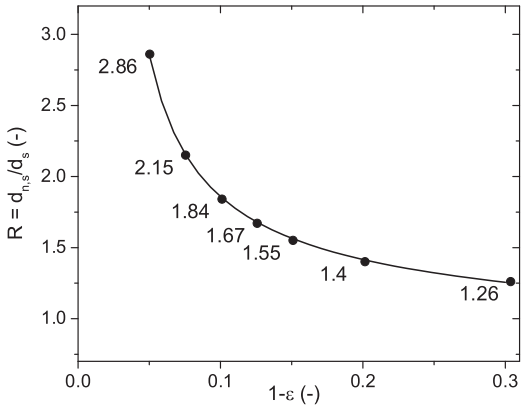

Fig. 2. Evolution of the ratio of the node to strut diameter estimated using the original TKKD model with parabolic strut profile [24] plotted against the foam solid fraction.

$$P_3 = \frac{d_s}{2} \tag{4}$$

where h is a geometrical constant equal to $h = 1 - cos(\gamma/2)$ (see [24] for further details), γ is the Plateu's angle (109.5°) and z_s is the axial coordinate of the junction between node and strut.

The definition of the strut diameter requires an additional constraint, which is identified in the amount of solid material loaded in the foam matrix. The same approach employed in [24] is adopted to impose the foam solid fraction. Struts with a ratio equal to 2 and 3 are displayed as examples in Fig. 1(c) and (d), respectively.

2.1.1.3. TKKD model with uniform strut diameter. A strut with uniform diameter along the axis, as shown in Fig. 1(b), can be obtained by dropping the condition of differentiability of the strut profile at the node junction. In fact, this constraint imposes a derivative of the strut profile at the node which leads to a degenerate and unphysical strut profile in the case of R = 1. Thus, a dedicated geometrical model is proposed for the generation of these foams. In particular, the TKKD model is modified by removing the differentiability constraint and by introducing a constant strut diameter. We consider the following assumptions:

- Tetrakaidekahedral unit cell.
- The solid material loaded in the structure is totally distributed between struts and nodes.
- Continuity of the strut profile and the strut/node junction.
- Equal node and strut diameters (R = 1).

The strut diameter along the axis is constant as shown in Eq. (6).

$$d(z) = d_s \tag{5}$$

As in the previous case, the strut diameter is finally calculated from the overall volume balance of the idealized foam cell.

2.2. Computational domain and numerical simulations of heat conduction

The definition of a proper meshing procedure is crucial for the accurate description of the heat transfer in open-cell foams. The computational domain of the sole solid phase is generated starting from the CAD file, obtained by the foam reconstruction procedure, by means of the snappyHexMesh utility of OpenFOAM framework [30]. This utility starts from a uniform background mesh, refines the region of the computational domain around the CAD surface using the cut-cell approach and, finally, snaps the mesh surface on the CAD file. Thus, the accurate reproduction of all the details of the foam geometries is guaranteed. Mesh convergence analysis has been carried out to obtain a solution independent from the computational domain. Several background meshes have been tested with high-quality refinement (three levels) along the foam surface. An influence of the mesh on the target quantity, i.e. the solid effective thermal conduction, below 1% is reached with a ratio between the strut diameter and the grid size of the background mesh equal to 3. This result was obtained on a small foam sample consisting of a cube of 3 cells per side to reduce the computational burden. The mesh is carefully generated to obtain high-quality grids with low non-orthogonality and skewness values.

The temperature distribution in the solid domain is evaluated by solving the steady Laplacian equation, Eq. (6):

$$\nabla(k_s \nabla T) = 0 \tag{6}$$

where T is the temperature of the solid and k_s the thermal conductivity of the solid material, which is herein assumed to be constant. A temperature gradient is imposed between the two opposite faces perpendicular to the considered axis, and adiabatic conditions are set on all the other surfaces. The finite volume method implemented in the OpenFOAM framework [30] has been employed for the solution of Eq. (6). A second order discretization scheme is employed for the Laplacian operator and the simulations are assumed to be converged when the residual is below 10^{-10}.

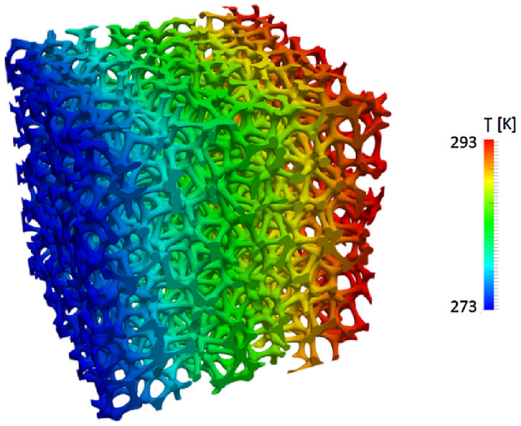

Fig. 3. Computational domain and temperature distribution in a foam with a porosity of 0.85, ΔT = 20 K.

The mono-directional stagnant effective thermal conductivity ($k_{eff,s}$) is then evaluated according to Eq. (7):

$$k_{eff} = \frac{-L \int_A J \, dA}{\Delta T \, S} \tag{7}$$

where J is the heat flux obtained from the simulation, A is the foam area where the temperature field is imposed, S is the area of the face of the computational domain, L and ΔT are the thickness of the sample and the temperature difference in the considered direction, respectively. Fig. 3 shows an example of a cubic computational domain for a foam with a porosity of 0.85, a cell size of 1.5 mm and a size of 7.5 cells per side.

3. Results and discussion

In this section, we discuss the results of the simulations of the 3D analysis of the heat conduction in the solid matrix.

3.1. Definition of the representative elementary volume

The analysis of the transport properties in open-cell foams requires the definition of a suitable representative elementary volume able to properly describe the structure behavior, as pointed out by Brun et al. [31]. The complex foam microstructure intrinsically presents local irregularities whose overall contribution becomes negligible when a sample larger than the representative element volume (REV) is considered. Thus, the definition of the REV is crucial to obtain a result independent from the size of the sample and, consequently, from the size of the computational domain. We numerically investigate virtually-reconstructed structures consisting of cuboids with side length equal to 3, 5, 7.5 and 9 open-cells to span a large range of sample dimensions. Fig. 4 shows that a representative elementary volume consisting of at least 7.5 foam cells is sufficient to achieve a sample-independent solution (variation below 1%).

This result is in contrast with the REV usually proposed in the literature, consisting of at least 3 cells in each direction [7,31], which comes from the analysis of the geometrical properties, i.e. specific surface area and porosity, and of the pressure drops, allowing for variations within 5%. Our analysis has confirmed that a REV of 3 cells is indeed sufficient to achieve a sample-independent description of the porosity. However, the tighter constraint on the maximum variation of the observed properties and particularly the strong dependence of the effective heat conductivity on the local structure explain the larger size

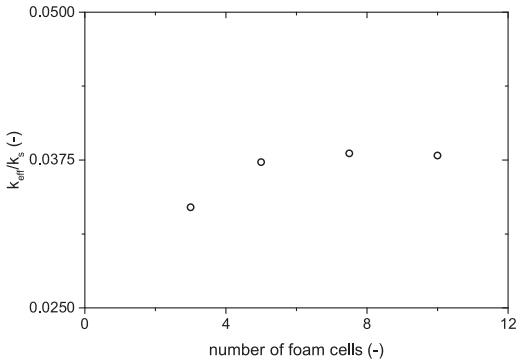

Fig. 4. Dimensionless effective thermal conductivity as a function of the representative elementary cell size.

of the required REV when dealing with Eqs. (6) and (7). Accordingly, the subsequent parametric analyses have been carried out by considering synthetic foam cuboids with side length larger than 7.5 foam cells.

3.2. Effect of the direction

The effect of the direction has been investigated to assess the isotropy of the virtually reconstructed foams. In this view, the effective thermal conductivities along three directions has been estimated for the same foam sample. Table 1 reports the results of this analysis. The effective thermal conductivity shows a very narrow distribution, with a spread of about 0.5%. This clearly confirms the isotropy of the virtually-generated structures, which also characterizes real foams [7]. Moreover, this is additional evidence that the selected REV is not affected by the local irregularities characteristic of the geometry.

3.3. Effect of cell size

To investigate the dependence on cell size, we generated foam samples with different cell diameters and we evaluated the effective thermal conductivity at different porosities. Fig. 5 shows the results for three different porosities. As expected, the cell size has a negligible effect on the effective thermal conductivity, in line with experimental measurements on ceramic [10] and metal [12] foams already reported in the literature. Thus, the dimension of the cell plays a minor role in the heat conduction mechanism in foams when the radiation contribution is neglected.

3.4. Effect of porosity

We investigate the effect of the porosity on the effective thermal conductivity of foams characterized by a broad range of void fractions between 0.7 and 0.95. As expected, the void fraction has a strong influence on the effective thermal conductivity, which increases with decreasing porosity, as shown in Fig. 6. By keeping constant the cell diameter, the strut diameter decreases with an increment of the porosity and, thus, the thermal resistance increases reducing the heat transfer efficiency. These simulation results are in line with the experimental measurements carried out on ceramic [10,14] and metal [11–14] foams. The comparison with the experimental data measured on foams with different cell size is enabled by the independence of the effective thermal conductivity from the cell size. The virtually-generated foams accurately describe the high porosity range and reasonably reproduce the behavior at lower porosity, where a scatter of the experimental data is observed.

The data collected in the region of high solid fractions are characterized by a high degree of uncertainty (up to 40%) as pointed out by Dietrich et al. [10]. In particular, the thermal conductivity of the ceramic solid material lays in a broad range of values depending on the manufacturing method and its accurate evaluation is not trivial. Moreover, the effect of the fluid embedded in these materials cannot be neglected when the conductivity of the solid is that of ceramic foams. Thus, the quantification of the separate contribution of the solid conduction relies on models which comprise some uncertainties and magnify the possible error of the experimental data.

Fig. 7 compares our effective thermal conductivity estimates with literature correlations. The effective thermal conductivities estimated with the Lemlich theory (Eq. (8)) [20] (curve a in Fig. 7), which is based on the analogy with electric conductivity, are in good agreement for foams with porosities larger than 0.9. This model is derived for the asymptotic condition of a unit void fraction, but it represents well the behavior of foams in a range of high porosities, which is typical of commercial metal foams. This result is confirmed by the numerical simulations of tomographically-reconstructed foams by Bianchi et al. [7].

$$\frac{k_{eff}}{k_s} = \frac{1-\varepsilon}{3} \tag{8}$$

A further decrement of the void fraction leads to more than linear increment of the effective thermal conductivity, resulting in an increased deviation from the Lemlich model [20], which strongly underestimates the results at low porosities. Lemlich proposed an additional model (Eq. (9)) [32] (curve b in Fig. 7) to overcome the limitation of the previous one, which does not respect the physical constraint of effective thermal conductivity equal to the solid conductivity at a unit solid fraction. This model, however, overestimates both the experimental data and numerical simulations.

$$6\frac{k_{eff}}{k_s} - 5\left(\frac{k_{eff}}{k_s}\right)^{4/3} + \left(\frac{k_{eff}}{k_s}\right)^{2} - 2(1-\varepsilon) = 0 \tag{9}$$

The effective thermal conductivity can be described by the expression in Eq. (10), as suggested by Freund and co-workers [25].

$$\frac{k_{eff}}{k_s} = \frac{1-\varepsilon}{\tau} \tag{10}$$

where ε is the void fraction and τ is a tortuosity parameter. Recently, Bianchi et al. [25] proposed a correlation for the tortuosity in periodic ordered structures (POCS) according to Eq. (11).

$$\tau = \frac{1}{(A(1-\varepsilon)+B)} \tag{11}$$

where A and B are fitting parameters evaluated from the regression of the simulations of heat conduction in the POCS structures. Since we are dealing with open-cell foams, we exploit the asymptotic results from Lemlich [20] and Maxwell [33] valid for porosity tending towards one and towards zero, respectively, to define the two parameters. The tortuosity of a foam structure is derived by Lemlich [20] in the case of high porosity, leading to:

$$\tau = 3 \quad \varepsilon \to 1 \tag{12}$$

The asymptotic result for the high solid fractions is derived by Maxwell [33] and is equal to:

$$\tau = 1 \quad \varepsilon \to 0 \tag{13}$$

By combining the two asymptotic behaviors in Eqs. (12) and (13),

Table 1
Effective thermal conductivity for three different directions for the sample having porosity equal to 0.9 and cell size equal to 1.5 mm.

Direction	k_{eff}/k_s [-]
x	0.0381
y	0.0383
z	0.0383

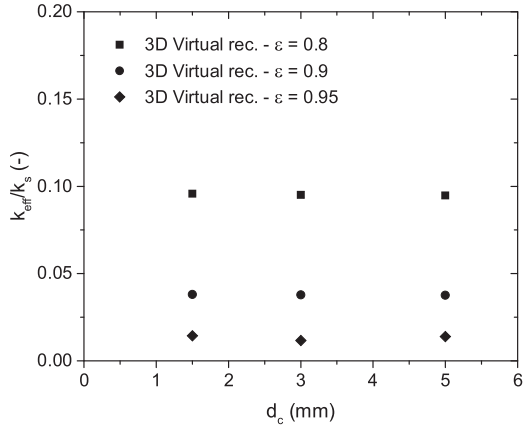

Fig. 5. Effect of cell diameters on the effective thermal conductivity at different porosities.

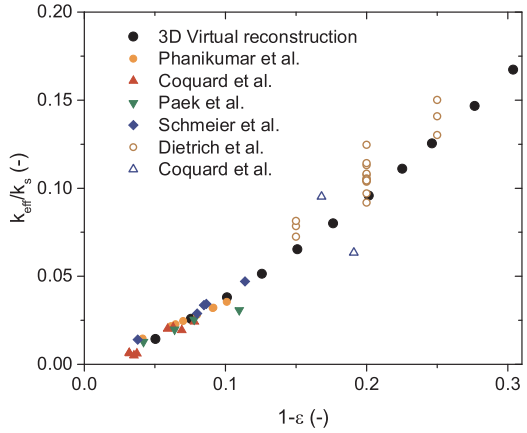

Fig. 6. Effective thermal conductivity evaluated for the virtually-generated foams with respect to the solid fraction compared with experimental data for ceramic [10,14] (open symbols) and metal (full symbols) foams [11–13].

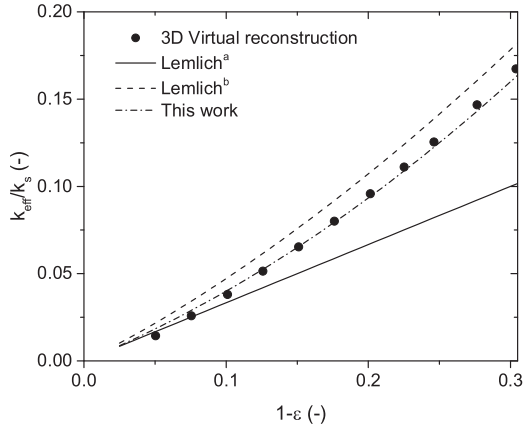

Fig. 7. Effective thermal conductivities estimated from the present numerical simulations on the virtually generated structures (full circle) compared with the Lemlich model (solid line – a, Eq. (8)) [20] and (dashed line – b, Eq. (9)) [32] and with the correlation proposed in this work (dash-dot line).

we obtain the correlation for the effective thermal conductivity reported in Eq. (14), where $A = 2/3$ and $B = 1/3$.

$$\frac{k_{eff}}{k_s} = \frac{1-\varepsilon}{\left(\frac{2}{3}(1-\varepsilon)+\frac{1}{3}\right)^{-1}} \tag{14}$$

It is worthwhile to notice that the values of A and B are in line with the ones proposed by Glicksman for closed-cell foams [34]. Eq. (14) is superimposed on the numerical simulations carried out on the virtually-reconstructed samples, as shown in Fig. 7. Thus, the hereby proposed correlation adequately describes the effective thermal conductivity of open-cell foams in a broad range of porosities without requiring any fitting parameters.

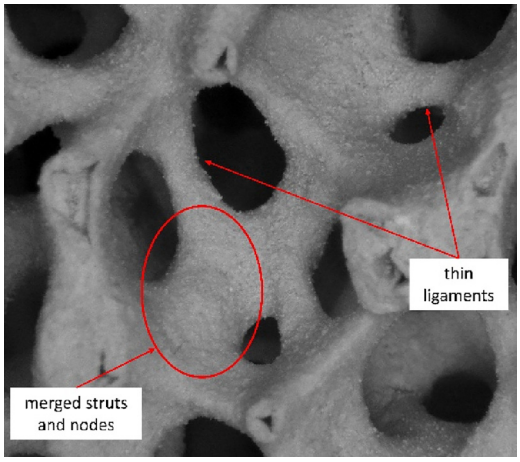

Fig. 8. Morphology of a low-porosity foam where the merging between strut and nodes is evident along with the presence of thin ligaments.

3.5. Effect of the ratio between node and strut diameters

Despite the fact that virtually-generated foams generally catch the trend of the experimental effective thermal conductivity, a significant scatter affects the experimental data in particular at low porosities, as shown in Fig. 6. As reported in Section 3.4, the degree of uncertainty of such measurements is high. An additional explanation of this trend is the very complex topological structure of foams in such conditions. In these structures, struts and nodes may merge together determining very large solid elements, whose presence is compensated by very thin ligaments which limit the heat conduction [35], as depicted in Fig. 8.

The reconstructed foams adopt a parabolic profile for the variation of the strut diameter along the axis, which results in a well-defined distribution of the solid material between struts and node. This assumption might not correspond to the real one in the low porosity range or, more generally, some specific manufacturing processes could generate foams with peculiar and different topological characteristics.

The effect of minor differences between the estimated diameters and the real ones have a minor influence on the prediction of the specific surface area, which was used for validating the original model in a wide range of parameters [21], but they are amplified in the analysis of the effective thermal conductivity. Thus, a parametric analysis of the effect of different distributions of the material between nodes and struts has been run by arbitrarily varying the ratio R between the node and strut diameters as already carried out by Freund and co-workers for ordered structures [25]. The foams are generated according to the virtual reconstruction procedure conveniently modified to deal with the different ratio R. In this view, the initial guesses for the node and strut diameters required by the method are evaluated using the modified versions of the TKKD model presented in Section 2.1.1.2 and 2.1.1.3. Then, the three-dimensional structures are generated using the virtual reconstruction starting from the same initial seeds. In this way, the skeleton of the reconstructed foams is the same, the only difference is the solid distribution between strut and nodes, governed by the ratio R. Moreover, the adjustment of the void fraction to a desired value which is the last step of the original reconstruction procedure has been skipped. In doing so, we are able to accurately describe the different ratios without the small alterations due to the adjustment procedure.

A higher ratio loads most of the solid in the nodes generating thin

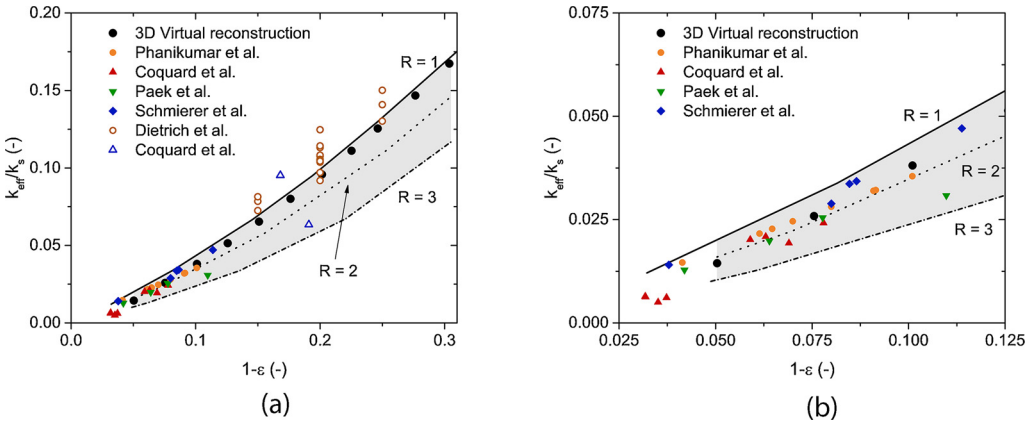

Fig. 9. Effective thermal conductivity at different porosities for virtually reconstructed foams and synthetic samples at different ratios between struts and nodes compared with experimental data for ceramic [10,14] (open symbols) and metal [11–14] (full symbols) foams.

struts. Conversely, a ratio tending to one places the solid mainly in the struts. Fig. 9 shows the results as a function of the porosity for three different ratios. A strong effect of the ratio on the effective thermal conductivity is obtained, as already reported for periodic ordered structures by Bianchi et al. [25]. The highest ratio strongly limits the heat conduction because of the small strut cross-sectional area, which is inversely proportional to the thermal resistance, see curve at R = 3 in Fig. 9. On the other hand, a unit ratio, i.e. constant cross-section along the strut axis, promotes the thermal conduction within the structure providing a much lower resistance to the heat flow, see curve at R = 1 in Fig. 9. The numerical results obtained for R = 1, i.e. the optimum structure, can be also seen as an upper boundary for the foam performances.

In this view, they can be used to distinguish among the experimental data the ones characterized by the largest uncertainties. Most of the experimental data fall within the envelope generated by the curves at different ratios. This is evidence of the complex topology of real foams structures, which are characterized by a broad spectrum of geometrical features. However, some experimental data for low porosity foams reports values higher than the ones predicted for the ideal node-strut distribution, i.e. R = 1, suggesting that they are likely affected by significant experimental error. At low solid fractions, the experimental data and the virtual foam models are aligned to the curve characterized by a ratio close to two (see Fig. 9b). This is confirmed by the tomographic measurements carried out by Bianchi et al. [7], where a ratio between struts and nodes equal to 1.72 was measured for a foam with porosity around 0.9. A similar ratio (1.84) is estimated by using the geometrical model by Ambrosetti et al. [24]. This model is employed in the virtual reconstruction to provide the initial guesses for node and strut diameters. In doing so, the final structure shows a void fraction which slightly deviates from the expected one. Thus, the surface of the foam is moved in order to obtain the required porosity, as described in [21]. However, the adjustments in the surface are small and the variations between the ratio of the ideal model and of the virtual foams are negligible. Thus, the agreement between the ratio evaluated by means of tomography and the one estimated in the virtually-generated foams assesses the adequacy of the reconstruction in accurately describing also the solid distribution in the structure. At lower porosities, the experimental data seem to be better represented by a ratio close to one. However, the small number of experimental data in this range and the high level of uncertainties (up to 40%) [10] does not allow for definitive conclusions. Overall, the reconstructed foams follow the experimental data quite well. This is due to the variable ratio between struts and nodes, which follows from the geometrical assumptions adopted in the derivation of the TKKD model employed for the initial estimation of the ligament diameters, as shown in Fig. 2.

3.6. Geometrical optimization of the foam structure

Additive manufacturing techniques are recently receiving growing attention as an alternative manufacturing route for ordered catalyst supports [26]. The very precise design of the final structure enabled by these methodologies can be exploited for the generation of optimized structures. Freund and co-workers [25] showed the capabilities of such approaches for the generation of optimized structures in the context of periodic ordered cellular structures. In this view, the results of this work elucidate the potential of the additive manufacturing also for the advanced design of disordered structures as open-cell foams. By focusing on high porosity metal foams, a strong improvement in the performances is expected by the accurate control of the geometry of the struts. In particular, the design of structure with a uniform strut diameter boosts the heat conductivity of such structures. It is worth to emphasize that the increase in the cross-sectional area of the strut at fixed porosity enables an increment of the effective heat conductivity between 20–30 %, as shown in Fig. 9. Moreover, a uniform strut diameter is expected to increase the specific surface area as well, as shown in Fig. 10, with a beneficial effect on the gas-to-solid mass and heat transfer rates, resulting in an additional improvement of the foam performances. As a drawback, the additional exposed surface slightly increases the pressure drops, which are function of the specific surface area at fixed porosity [3].

According to our analysis, the potential of these supports is strongly boosted by adjusting the geometry of the struts preserving the other characteristics. At low porosity, the improvement reached using the

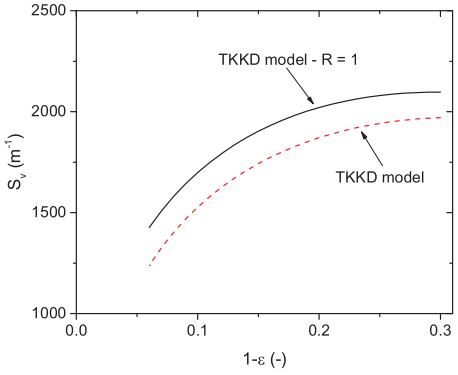

Fig. 10. Evaluation of the specific surface area for a foam with d_c = 1 mm for the original TKKD model [24] (red dashed line) and for the TKKD model modified with R = 1 (black solid line) (For interpretation of the references to colour in this figure legend, the reader is referred to the web version of this article).

optimized structures is negligible because the foams diameter ratio between ligaments and nodes is already around one. However, the current commercial foams in this range of void fraction are made of ceramic materials, whose intrinsic conductivity is poor. In this context, the virtually-generated structures allow for the generation of novel real structures manufactured in conductive metals, thus paving the way to the application of low porosity metal foams characterized by sufficiently high effective thermal conductivity. In this view, the virtual generation procedure, proposed in [21] and modified in this work, becomes a valid design tool able to generate highly optimized foams directly providing CAD files of the structures ready to be built with additive manufacturing techniques.

4. Conclusions

In this work we have extensively analyzed the effective solid thermal conductivity of open-cell foams by means of 3D simulations on virtually-generated foam samples. A negligible dependence on the cell diameter is found. The effective thermal conductivity of open-cell foams strongly depends on the void fraction at fixed cell size. On decreasing the porosity at constant cell diameter, in fact, the strut cross-sectional area increases, providing less resistance to the heat conduction. These results are valid for the pure heat conduction, whereas the conjugate problem in presence of convective gas-to-solid heat transfer is influenced also by geometrical properties which depend on the cell size.

Our results further show that the effective thermal conductivity strongly depends on the solid distribution between node and struts and along the strut axis. The effect of different distributions has been investigated by changing the ratio between node and strut diameters. This analysis elucidates that a reduction of the strut cross-sectional area at constant void fraction penalizes the thermal conduction, the performance decays depending on the ratio between node and strut diameters. A high ratio implies a small cross-sectional strut area with most of the solid material loaded in the nodes, resulting in a poor effective thermal conductivity. As expected, the analysis also revealed that the best heat transfer performances are obtained in the case of a uniform strut cross-section, in line with the findings of Bianchi et al. for periodic ordered structures [25]. We estimate an improvement between 20 and 30% over existing typical open-cell foams with porosities greater than 0.9. Thus, the thermal properties of these structures can be significantly enhanced preserving the other beneficial properties of open-cell foams. Notably, common manufacturing techniques produce open-cell foams without control on the distribution of the material, thus preventing the generation of optimal structures. In this context, additive manufacturing techniques show an enormous potential in providing real structures generated with the highest degree of optimization [25]. In this view, the virtual generation procedure recently proposed [21] and herein modified to manage variable node/strut ratios is a valid tool for the advanced design and manufacturing of optimized open-cell foams. The virtual generation procedure is able to provide CAD files ready for the additive manufacturing techniques, i.e. 3D printing, removing the limitations in the microstructure of open-cell foams imposed by the current commercial manufacturing technologies.

On a more methodological basis, this work elucidates the capability of the virtually-generated structures to mimic the average behavior of real open-cell foams, enabling the fundamental investigation of their transport properties. Furthermore, it clearly shows the potential of such an approach in the optimization and design of these structures, thus paving the way for the generation of enhanced catalyst substrates tailored to the process requirements.

Acknowledgements

The research leading to these results has received funding from the European Research Council under the European Union's Horizon 2020 research and innovation programme (Grant Agreement no. 694910/INTENT). Computational time at CINECA (Bologna) is gratefully acknowledged.

References

[1] E. Tronconi, G. Groppi, C.G. Visconti, Structured catalysts for non-adiabatic applications, Curr. Opin. Chem. Eng. 5 (2014) 55–67, http://dx.doi.org/10.1016/j.coche.2014.04.003.
[2] J. Gascon, J.R. van Ommen, J.A. Moulijn, F. Kapteijn, Structuring catalyst and reactor – an inviting avenue to process intensification, Catal. Sci. Technol. 5 (2015) 807–817, http://dx.doi.org/10.1039/C4CY01406E.
[3] A. Inayat, M. Klumpp, M. Lämmermann, H. Freund, W. Schwieger, Development of a new pressure drop correlation for open-cell foams based completely on theoretical grounds: taking into account strut shape and geometric tortuosity, Chem. Eng. J. 287 (2016) 704–719, http://dx.doi.org/10.1016/j.cej.2015.11.050.
[4] L. Giani, G. Groppi, E. Tronconi, Mass-transfer characterization of metallic foams as supports for structured catalysts, Ind. Eng. Chem. Res. 44 (2005) 4993–5002, http://dx.doi.org/10.1021/ie0490886.
[5] L. Giani, G. Groppi, E. Tronconi, Heat transfer characterisation of metallic foams, Ind. Eng. Chem. Res. 44 (2005) 9078–9085.
[6] V.V. Calmidi, R.L. Mahajan, Forced convection in high porosity metal foams, J. Heat Transfer 122 (2000) 557–565, http://dx.doi.org/10.1115/1.1287793.
[7] E. Bianchi, T. Heidig, C.G. Visconti, G. Groppi, H. Freund, E. Tronconi, An appraisal of the heat transfer properties of metallic open-cell foams for strongly exo-/endothermic catalytic processes in tubular reactors, Chem. Eng. J. 198–199 (2012) 512–528, http://dx.doi.org/10.1016/j.cej.2012.05.045.
[8] P. Aghaei, C.G. Visconti, G. Groppi, E. Tronconi, Development of a heat transport model for open-cell metal foams with high cell densities, Chem. Eng. J. 321 (2017) 432–446, http://dx.doi.org/10.1016/j.cej.2017.03.112.
[9] A. Montebelli, C.G. Visconti, G. Groppi, E. Tronconi, C. Ferreira, S. Kohler, Enabling small-scale methanol synthesis reactors through the adoption of highly conductive structured catalysts, Catal. Today 215 (2013) 176–185, http://dx.doi.org/10.1016/j.cattod.2013.02.020.
[10] B. Dietrich, G. Schell, E.C. Bucharsky, R. Oberacker, M.J. Hoffmann, W. Schabel, M. Kind, H. Martin, Determination of the thermal properties of ceramic sponges, Int. J. Heat Mass Transfer 53 (2010) 198–205, http://dx.doi.org/10.1016/j.ijheatmasstransfer.2009.09.041.
[11] E.N. Schmierer, A. Razani, Self-Consistent open-celled metal foam model for thermal applications, J. Heat Transfer 128 (2006) 1194, http://dx.doi.org/10.1115/1.2352787.
[12] J. Paek, B. Kang, S. Kim, J. Hyun, Effective thermal conductivity and permeability of aluminum foam materials, Int. J. Thermophys. (2000) 453–464, http://dx.doi.org/10.1023/A:1006643815323.
[13] M.S. Phanikumar, R.L. Mahajan, Non-Darcy natural convection in high porosity metal foams, Int. J. Heat Mass Transfer 45 (2002) 3781–3793, http://dx.doi.org/10.1016/S0017-9310(02)00089-3.
[14] R. Coquard, D. Rochais, D. Baillis, Experimental investigations of the coupled conductive and radiative heat transfer in metallic/ceramic foams, Int. J. Heat Mass Transfer 52 (2009) 4907–4918, http://dx.doi.org/10.1016/j.ijheatmasstransfer.2009.05.015.
[15] V.V. Calmidi, R.L. Mahajan, The effective thermal conductivity of high porosity fibrous metal foams, J. Heat Transfer 121 (1999) 466, http://dx.doi.org/10.1115/1.2826001.
[16] A. Bhattacharya, V.V. Calmidi, R.L. Mahajan, Thermophysical properties of high porosity metal foams, Int. J. Heat Mass Transfer 45 (2002) 1017–1031, http://dx.doi.org/10.1016/S0017-9310(01)00220-4.
[17] X. Fan, X. Ou, F. Xing, G.A. Turley, P. Denissenko, M.A. Williams, N. Batail, C. Pham, A.A. Lapkin, Microtomography-based numerical simulations of heat transfer and fluid flow through β-SiC open-cell foams for catalysis, Catal. Today 278 (2016) 350–360, http://dx.doi.org/10.1016/j.cattod.2015.12.012.
[18] J. Randrianalisoa, D. Baillis, C.L. Martin, R. Dendievel, Microstructure effects on thermal conductivity of open-cell foams generated from the Laguerre–Voronoï tessellation method, Int. J. Therm. Sci. 98 (2015) 277–286, http://dx.doi.org/10.1016/j.ijthermalsci.2015.07.016.
[19] P. Ranut, On the effective thermal conductivity of aluminum metal foams: review and improvement of the available empirical and analytical models, Appl. Therm. Eng. 101 (2016) 496–524, http://dx.doi.org/10.1016/J.APPLTHERMALENG.2015.09.094.
[20] R. Lemlich, A theory for the limiting conductivity of polyhedral foam at low density, J. Colloid Interface Sci. 64 (1978) 107–110, http://dx.doi.org/10.1016/0021-9797(78)90339-9.
[21] M. Bracconi, M. Ambrosetti, M. Maestri, G. Groppi, E. Tronconi, A systematic procedure for the virtual reconstruction of open-cell foams, Chem. Eng. J. 315 (2017) 608–620, http://dx.doi.org/10.1016/j.cej.2017.01.069.
[22] G.L. Vignoles, A. Ortona, Numerical study of effective heat conductivities of foams by coupled conduction and radiation, Int. J. Therm. Sci. 109 (2016) 270–278, http://dx.doi.org/10.1016/j.applthermaleng.2015.09.094.
[23] S. Cunsolo, R. Coquard, D. Baillis, N. Bianco, Radiative properties modeling of open cell solid foam: review and new analytical law, Int. J. Therm. Sci. 104 (2016) 122–134, http://dx.doi.org/10.1016/j.ijthermalsci.2015.12.017.
[24] M. Ambrosetti, M. Bracconi, G. Groppi, E. Tronconi, Analytical geometrical model of open cell foams with detailed description of strut-node intersection, Chemie-Ingenieur-Technik 89 (2017), http://dx.doi.org/10.1002/cite.201600173.
[25] E. Bianchi, W. Schwieger, H. Freund, Assessment of periodic open cellular

structures for enhanced heat conduction in catalytic fixed-bed reactors, Adv. Eng. Mater. 18 (2016) 608–614, http://dx.doi.org/10.1002/adem.201500356.
[26] M. Klumpp, A. Inayat, J. Schwerdtfeger, C. Körner, R.F. Singer, H. Freund, W. Schwieger, Periodic open cellular structures with ideal cubic cell geometry: effect of porosity and cell orientation on pressure drop behavior, Chem. Eng. J. 242 (2014) 364–378, http://dx.doi.org/10.1016/j.cej.2013.12.060.
[27] C. Kloss, C. Goniva, A. Hager, S. Amberger, S. Pirker, Models, algorithms and validation for opensource DEM and CFD-DEM, Prog. Comput. Fluid Dyn. 12 (2012) 140–152, http://dx.doi.org/10.1504/PCFD.2012.047457.
[28] J.A.F. Plateau, Experimental and Theoretical Static of Liquids Subject to Molecular Forces Only, (1873).
[29] A. Liebscher, C. Redenbach, Statistical analysis of the local strut thickness of open cell foams, Image Anal. Stereol. 32 (2013) 1–12, http://dx.doi.org/10.5566/ias.v32.p1-12.
[30] H. Jasak, A. Jemcov, Z. Tukovic, OpenFOAM : A C + + library for complex physics simulations, Int. Work. Coupled Methods Numer. Dyn. (2007), pp. 1–20.
[31] E. Brun, J. Vicente, F. Topin, R. Occelli, M.J. Clifton, Microstructure and transport properties of cellular materials: representative volume element, Adv. Eng. Mater. 11 (2009) 805–810, http://dx.doi.org/10.1002/adem.200900131.
[32] R. Lemlich, Semitheoretical equation to relate conductivity to volumetric foam density, Ind. Eng. Chem. Process Des. Dev. 24 (1985) 686–687, http://dx.doi.org/10.1021/i200030a027.
[33] J.C. Maxwell, A Treatise on Electricity and Magnetism, 3rd ed., (1892) Oxford.
[34] L.R. Glicksman, Heat transfer in foams, in: N.C. Hilyard, A. Cunningham (Eds.), Low Density Cell. Plast. 1st ed., Springer, Netherlands, 1994, p. 369.
[35] G. Incera Garrido, F.C. Patcas, S. Lang, B. Kraushaar-Czarnetzki, Mass transfer and pressure drop in ceramic foams: a description for different pore sizes and porosities, Chem. Eng. Sci. 63 (2008) 5202–5217, http://dx.doi.org/10.1016/j.ces.2008.06.015.